Acoustics'08 Paris
June 29-July 4, 2008
www.acoustics08-paris.org

Effects of filtering of room impulse responses on room acoustics parameters by using different filter structures

Csaba Huszty, Norbert Bukuli, Ákos Torma and Fülöp Augusztinovicz

Budapest University of Technology and Economics, BME Dept. of Telecommunications,
Magyar tudósok körútja 2, H-1117 Budapest, Hungary
huszty@hit.bme.hu

Room acoustic evaluation is usually based on post-processing of measured room impulse responses (RIRs), and this often requires some kind of filtering, for instance to derive fractional octave band parameters of a room. In this paper it is shown that the considerable variance of room acoustic parameters of almost any hall is partly caused by the filtering method and the filter properties used in the course of post-processing. The paper proposes new qualification methods and parameters for determining the quality of FIR filter banks, taking their use for acoustic evaluation into account. It suggests practical considerations for the design as well, and shows the analysis and comparison of effects of various filter properties – such as filter types and topology structures – on some room acoustics parameters. By using the suggested methods, it is possible to derive more accurate and reliable results in room acoustic evaluation.

1 Introduction

Sub-band room acoustic parameters are calculated by filtering wideband room impulse responses (RIRs) into different frequency bands with a given bandwidth, such as 1/3 octave bands. The filter quality parameters are defined in standards [1], but they are mostly based on the analogue filter design rules for Infinite Impulse Response (IIR) filters. However, recent techniques include other filters as well, such as Finite Impulse Response (FIR) filters or Wavelet filters. There are three main properties of a filter that affects room acoustic parameters: the frequency, the temporal and the energetic properties. We think that the common finding that room acoustics parameters are prone to a higher variance at lower frequencies [3], is partly caused by the filtering methods and filter bank properties themselves. It was previously discussed [5, 6, 4] that a particular filter can be used for room acoustic evaluation only if it satisfies the criterion $BT_{60} > 16$ (B: bandwidth, T_{60}: room reverberation time). This applies very well for causal filters used in realtime applications such as Butterworth filter banks, however offline RIR-processing allows using acausal filters as well, either based on truncated Butterworth filters by forward-backward-filtering, or other filters such as Wavelets [5, 6], leading to linear-phase results, which is a great advantage, as $BT_{60} > 4$ is also sufficient then. In this work we present a comparison of the different filter structures.

2 Test environment

To evaluate different filtering techniques and room acoustic parameters, we designed an artificial room impulse response (ARIR) that is based on a random white Gaussian noise with a crest factor of 4.2, simulating a small yet diffuse sound field. As the filtering process disrupts evaluation results at small enclosures such as a car interior, we set the reverberation time to 0.1 s on an 1 second long sample, with a sampling rate of $f_s = 48$ kHz. Although a real world RIR has a narrowing bandwidth over time, we used a wideband reverberation model.

2.1 Test repeatability

We use a stochastic signal to model the tail part so we have to test different realizations of the ARIR and examine the expected value of the estimated RT60 by means of ensemble averaging – we assume that the reverberation tail is an ergodic process for simplicity. We used a sufficient number of 2000 different ARIR representations for each RT60 time estimation phase.

2.2 Room acoustic parameters

In this present work we chose to test the estimation of the RT60 reverberation time from the traditional temporal room acoustic parameters (such as RT60, RT10, RT20, RT30, EDT10, EDT15, BR, TR, etc.). Temporal parameters have the common feature of being calculated from the Energy Decay Curve (EDC), which may be greatly affected by the filtering. Other parameters are also affected, but they will be presented in a forthcoming work.

3 Filter bank requirements

The ANSI specification [1] defines 3 different classes of filters with tolerance schemes; Class 0 has the best quality. The parameters and formulae given therein are valid up to a 1/3 octave band resolution, so we chose to test filter banks with this resolution.

3.1 Sum and phase response of sub-bands

For a complete decomposition of the wideband signal, the sub-bands have to have a flat magnitude response if summarized. However in order to avoid dispersion – frequency dependent time shift –, it is also essential to conduct linear-phase filtering when evaluating acoustic parameters. Linear-phase filtering introduces latency as such filters have symmetrical impulse responses.

3.2 Decay and pre-ringing of the filter

There are two main problems when the decay of the filter impulse response is remarkably slow. Firstly it lengthens the RIR, which can be a problem when small enclosures have a comparable RIR length to the filter length. Secondly, the smoothness of the filter decay correlates with providing a smoothly decaying filtered RIR, a must for accurate RT60 estimations. When there is a lack of smoothness, the effect is referred to as the 'warble' effect. We conclude the aim of finding the least length and smoothest decaying filter that is possible.

3.2.1 Warble effect of the filtered EDC

The warble effect of a filtered EDC corrupts RT estimations in a level-dependent way (e.g. different for RT10 or RT20). Warbling is caused by uneven distribution of arriving energy at the decay part leading to a staggered EDC. Due to warbling assumptions of the ISO standard [2] for determining regression points at the diffuse field is violated. We propose here detecting and quantifying the warbling by using the R^2 coefficient of determination on an F_{EDC_i} line fitted to the warbled EDC EDC_i by robust multilinear regression [7] that efficiently handles outlier samples. We can calculate this coefficient as follows:

$$R^2 = \frac{\sum_i (F_{EDC_i} - \overline{EDC})^2}{\sum_i (EDC_i - \overline{EDC})^2} \quad (1)$$

$\overline{EDC}$ is the average of the EDC values. An R^2 of 1.0 indicates a perfect fit, therefore we define the W warble on a 0 (no warble) to 10 (unable to fit) scale as:

$$W = 10 \cdot (1 - R^2) \quad (2)$$

3.2.2 Shape change of the filtered EDC

According to the discrete convolution formula, the length of the filtered RIR will be $L_{fFIR} = L_{RIR} + L_{FIR} - 1$ where L_{RIR} is the length of the RIR and L_{FIR} is of the applied filter. This means the RT60 will be systematically overestimated because the filter will further 'reverberate' the RIR making it longer. The lengthened EDC of a filtered band is:

$$\begin{aligned} &EDC_{band}(t) = \\ &= 10\log_{10}\frac{\int_t^\infty \int_{-\infty}^\infty h_{RIR}(\tau)h_{FILT}(t-\tau)\,d\tau dt}{\int_{-\infty}^\infty \int_{-\infty}^\infty h_{RIR}(\tau)h_{FILT}(t-\tau)\,d\tau dt} \end{aligned} \quad (3)$$

and the overestimation for the T_k reverberation time for estimation level k is

$$\begin{aligned} \Delta T_k = \frac{60}{k}(&\Delta \arg\{EDC(t) = -(k+5)\} - \\ &-\Delta \arg\{EDC(t) = -5\}) \end{aligned} \quad (4)$$

where Δ means difference. It shall be noted that a simplified closed form of Eq. 4 is yet to be found. The authors believe that a compensation may be possible with the above formulae taking into account that the factor of overestimation should be determined case-by-case for each band of the filter bank. Similarly, a compensation might be done by calculating the RT60 of the filters (without using a regression model) and subtract it from the filtered EDC, differently for each k estimation levels.

3.2.3 Shift of the filtered EDC

Despite of lengthening the reverberation process, applying linear-phase filters introduce an energy shift in the starting point of the EDC when the time of arrival (TOA) of the original and filtered direct sound is synchronized. This is because linear-phase filters have symmetrical filter impulse responses and they introduce a latency of $GD/2$ (GD is the group delay) which is compensated by truncating the data before $GD/2$. This truncation removes the preceding energy and therefore will down-shift the initial level of $EDC(t) = 0$ dB even if the direct sound was arriving at $t > 0$. When calculating energetic room acoustic parameters, this has to be taken into account, therefore we suggest extending the time limits backwards to $-GD/2$ without truncation. This is in good agreement with the solution for overcoming on nonlinear-phase time domain smearing by first splitting the RIR and then filtering it and extending the time limits according to the delay of the filter, as described in [2].

4 Filter bank implementations

Besides the direct band-pass filter (BPF) realization of filter banks, there are other methods which we present and compare here.

4.1 Cascaded filter structures

In order to have a completely flat sum of bands, it is more efficient to use filter banks consisting of cascaded high-pass (HPF) or low-pass (LPF) filters. The signal is filtered with the filter of the first stage and then at the following stages, the differences are filtered again, thus the signals of the band-pass sub-bands are produced. In order to use such filtering structures, high-quality filters have to be designed as errors are prone to spread and develop due to the reuse of the filtered results.

4.2 Multirate filtering

When it is not possible to design filters any more due to computational limits or convergence problems, one of the possible methods to overcome is multirate filtering. Instead of narrowing a frequency band of a filter, we expand the signal in the frequency domain by changing its sampling frequency After that we reconstruct the original sampling frequency by interpolation. This method is efficient only if the bandwidth of the source signal is practically narrow enough, because otherwise the interpolation filter is the one that is difficult to design. When implementing fractional octave filtering with this technique, the signal should be widened in the frequency scale in a non-integer value, therefore a rational fractional pair of numbers shall be found for the decimation and the interpolation (see block diagram on Fig. 1. For example, when 1/3 octave band filtering is employed, the approximation of $\sqrt[3]{2} \cong 5/4$ can be used. However, this causes a minor shift of the band center frequencies, which may lead to more strict design rules when trying to be compliant with the ANSI classification requirements.

4.3 Wavelet filtering

Unlike using the exponential eigenfunction as a basis of spectral decomposition of a signal, it is possible to use wavelets instead and construct new filter banks with better characteristics. Wavelets are finite length functions that are constructed to be optimal for given tasks. The filtering is realized by scaling the wavelet function because wavelets are band-limited. One of the main advantages of utilizing wavelet filters is that they can be designed to have constant bandwidth conveniently. Using symmetric wavelets results in linear-phase filtering which is a further advantage. In this present approach, the Continuous Wavelet Transform (CWT) is used with

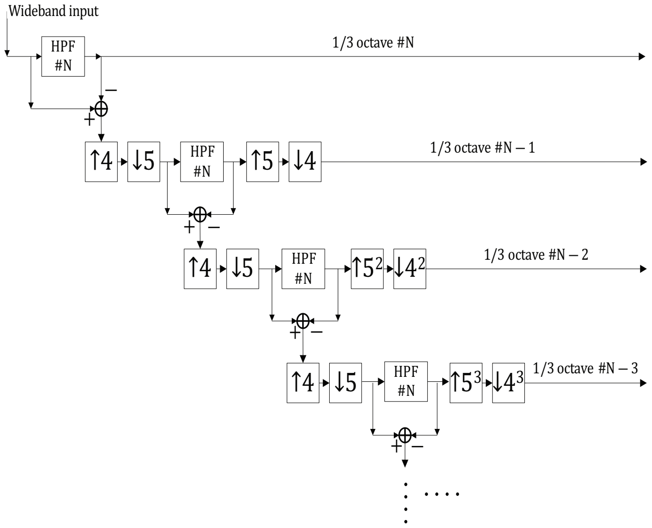

Figure 1: 1/3 octave-band filter bank block diagram utilizing multirate filtering based on cascaded high-pass filters (HPF). One possible implementation.

a discrete set of scale factors in order to have a finite number of results. We compared Mexican Hat, Meyer, Modified Morlet, Shannon and Harmonic wavelets and found that the Modified Morlet wavelet produces the best results due to its exponential decay as also presented by [5, 6]:

$$\Psi(t) = K \cdot e^{j2\pi f_c t \frac{-t^2}{2\sigma^2}} \tag{5}$$

which is a sine function multiplied by a Gauss-function. f_c denotes the center frequency, K is a constant for energy normalization and the bandwidth of the filter is $\sigma = 1/B$. Wavelet filters however might suffer a bad separation between the bands and the scaling factors have to be set precisely case-by-case in order to have the sum of the bands nearly constant.

5 Evaluation and results

In order to evaluate the quality of IIR, FIR and Wavelet filters, we first implemented the tolerance schemes of the ANSI specification [1] and classified the filter banks. A filter bank class was determined by selecting the class of its worst band. To determine the class of a band, we compared the $|S_+(j\omega)|$ and $|S_-(j\omega)|$ lower and upper magnitude tolerance scheme with the actual filter magnitude $|H(j\omega)|$ and defined a relative error based on their difference as follows:

$$h_{lower} = \int_{-\infty}^{\infty} \mathbf{P}\left\{|S_-(j\cdot\omega)| - |H(j\cdot\omega)|\right\}\, d\omega \tag{6}$$

$$h_{upper} = \int_{-\infty}^{\infty} \mathbf{P}\left\{|H(j\cdot\omega)| - |S_+(j\cdot\omega)|\right\}\, d\omega \tag{7}$$

$$E = \frac{h_{upper} + h_{lower}}{\int_{\omega_l}^{\omega_u} 1\, d\omega} \tag{8}$$

where $\mathbf{P}$ is an operator that separates the positive part of the difference; ω_u is the upper and ω_l is the lower circular frequency of the band. Results are shown in Table 1.

5.1 Evaluation of IIR filters

We evaluated one of the most common filters, the Butterworth (maximally flat) type, which is often used with low orders (e.g. 3-6). Common properties of an order N Butterworth filter is that its transition-band attenuation steepness equals to $-N \cdot 20\frac{\mathrm{dB}}{\mathrm{decade}} = -N \cdot 6\frac{\mathrm{dB}}{\mathrm{octave}}$; its pass-band ripple is minimal (maximally flat property) but its phase response is non-linear.

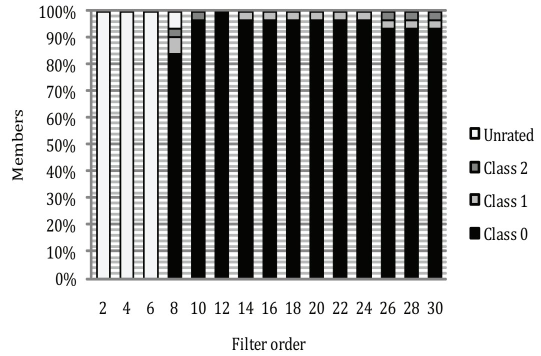

Figure 2: ANSI classification of Butterworth IIR filters of different orders. Relative number of members per ANSI classes versus filter order is shown.

We can see that only order 12 Butterworth filters are Class 0 compliant for 1/3 octave band analysis, and increasing the order does not help, as the filters become more steep, some of them will violate the pass-band minimum tolerance scheme making the whole bank fall to higher classes (lower quality).

5.2 Evaluation of FIR filters

5.2.1 Windowed filters

Windowed FIR filters are designed by time-windowing an impulse response of a filter having an idealistic magnitude curve. Windowed filters can be designed to be linear-phase but their magnitude is different according to the window. We designed windowed filters of different orders with different windows and tested their ANSI class compliance and we also evaluated the quality of these filters by using the above proposed methods. We conclude that in order to design Windowed filters to be partly ANSI compliant, higher orders are necessary. Higher order filters however corrupt the EDC curve more. It seems that Windowed filters are not appropriate for room analysis, although they have linear phase response and are very easy and fast to design. Results are shown in Table 1.

5.2.2 Equiripple filters

Equiripple filters have pre-defined maximum amplitude of pass-band and stop-band magnitude ripple and they usually have linear-phase response. They are however very difficult to design compared to Windowed filters for a reason which is out of the scope of this work, but this results in having great difficulties in designing ANSI-compliant filters at lower frequencies, even in the presented cascaded HPF or LPF topology. The authors were not able to design BPF Equiripple filters for 1/3 octave band, but HPF filters were successfully designed from band 22 (out of the 30 1/3 octave bands).Missing bands of 1-21 were generated with the multirate-technique. Despite these difficulties, a particular filter bank should only be designed once for a given sample rate so equiripple filters are still usable. They actually performed better than Butterworth filters; detailed evaluation results are shown in Table 1.

5.3 Evaluation of FIR filter bank design

In this section we propose new parameters for the evaluation of filter design.

5.3.1 Attenuation surface

It often occurs during that the filter bank design is unsuccessful due to convergence or the quality problems. Therefore to evaluate a designed filter bank at a first glance, we propose to plot the 'attenuation surface', which is a three dimensional plot showing the resulting stop-band attenuation in the function of frequency and the required stop-band attenuations.

5.3.2 Stop-band gravity frequency and relative crosstalk

It is preferred to achieve as good separation of the subbands as possible, as a bad separation results in a blurred parameter estimation, although the resolution (the number of bands) remains unchanged. To quantify the amount of separation, we propose introducing the stop-band gravity frequency from which we can calculate the relative overlap of the bands. For cascaded filters where only one stop-band exists, the stop-band gravity frequency ω_{grav} is the frequency that corresponds to the center-of-gravity of the $\mid H(j\omega)\mid$ magnitude of a given filter. The stop-band for a filter starts from the band-limiting frequency ω_{limit} and ends at the stop-band frequency ω_{stop} which is, for example the -3 dB point of the magnitude. So in other words, ω_{grav} is the solution of Eq.9.

$$\omega_{grav} : \int_{\omega_{limit}}^{\omega_{grav}} |H(j\omega)|\, d\omega = \frac{1}{2}\int_{\omega_{grav}}^{\omega_{stop}} |H(j\omega)|\, d\omega \quad (9)$$

The relative crosstalk c_{rel} is the distance of the stop-band gravity frequency from the stop-band frequency normalized by the center frequency of the selected band. The normalization allows us to compare bands with different bandwidth.

$$c_{rel} = \frac{|\omega_{stop} - \omega_{grav}|}{\omega_{center}} \quad (10)$$

This number quantifies the separation, because it relies on two main properties: the slope of the transitive band, and the flatness of the stop-band. It can be seen that if either the slope of declination or the attenuation over distant frequencies decreases, the distance of the stop-band gravity frequency and the stop-band frequency will increase. We can use this parameter for many purposes including comparing filter banks and determining another set of optimal parameters for filter bank design.

5.3.3 Filter order surface

When using an FIR filter bank in practice, we would like to have its filters at the least possible order, because shorter filters make a filter bank perform faster and require less computational and storage resources, and also reduce the amount of time-domain smearing. To visualize what minimum possible order filters a particular filter bank design algorithm produces, we propose plotting the order number as a function of sub-band center frequency and stop-band attenuation.

5.4 Evaluation of Wavelet filters

Reverberation time of two different decayed random noise based artificial impulse responses analyzed with a Modified Morlet (MM) Wavelet filter bank of 1/3 octave band. We have found that for short reverberation times, the repeatability of the measurements are bad, and the deviation of the results of the reverb time estimation is dependent on the regression algorithm (Fig. 3).

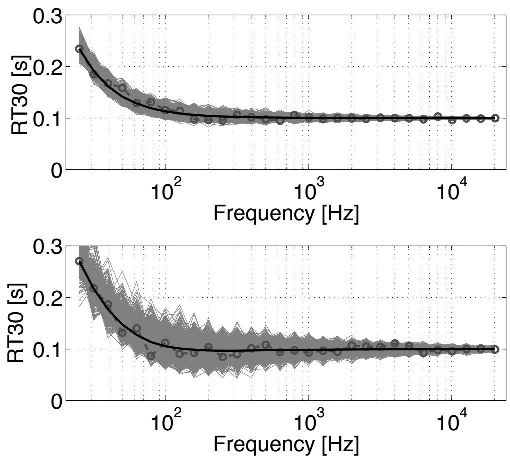

Figure 3: RT_{30} of 2000 representations (grey) of a $RT_{60} = 0.1$ s artificial room impulse response (ARIR) using 1/3 octave band MM Wavelet filter bank. Upper graph: robust multilinear [7], lower graph: linear regression [2] estimation. Solid line: expected value, dashed line: 1 selected representation.

6 Conclusion

We have found that the filtering process may significantly affect the evaluated room acoustic parameters - such as the reverberation time - especially in small enclosures. Filter impulse responses should have a prompt and smooth decay in order to avoid overestimation of the reverberation time and warble in the decay, respectively. To avoid dispersion of energy, linear-phase response and group delay compensation is needed for accurate estimation of the energetic room acoustic parameters. We proposed extending the time limits for energetic room acoustics parameters backwards according to the half of the filter group delay. Compensation for reverberation time estimation errors and the detection and quantification of the warbling effect was introduced together with new filter bank design evaluation parameters. Following the design of several different filter banks, an arti-

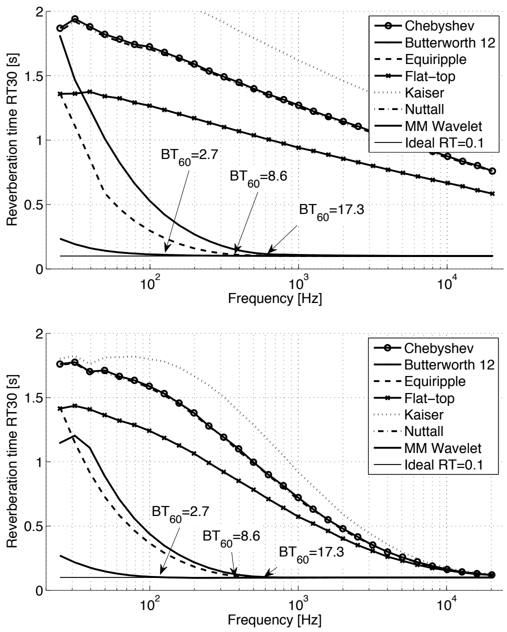

Figure 4: Expected values of reverberation times of an $RT_{60} = 0.1$ s artificial room impulse response (ARIR) for different filter structures. 2000 representations were ensemble averaged. Top: Robust multilinear regression, Bottom: ISO 3382 regression.

ficial room impulse response was processed and it was found that Equiripple FIR filters and Modified Morlet (MM) Wavelet affected the reverberation time estimation the least. Other structures, such as the commonly used Butterworth filters or Windowed FIR filters introduced high estimation errors (see Fig 4). Equiripple filters provide excellent separation but they are difficult to design, while MM Wavelet filters are not ANSI compliant but are easy to design. We found that filtering with MM Wavelet filters is possible at low as $B \cdot T_{60} = 3$ when ensemble averaging is used. It may further improve the estimation if more complex regression methods are used - such as the robust multilinear regression [7] - compared to the linear regression method of the [2] standard. The minimum required reverberation times at the lowest frequency for accurate 1/3 band analysis was presented for the above mentioned filters. It was an interesting result to find that extending the order of the FIR filters does not improve their ANSI compliance because of violating the tolerance curves at the pass-band, although their properties of separation advance. The authors believe consequently that the ANSI specification was created for Butterworth IIR filters and might need to be updated for other filter structures.

Type and topology	Order	Class 0 bands	Max. error [dB]	$\overline{W}$	RT_{min} [s]
Butterw. IIR BPF	12	all	$-\infty$	0.29	2.53
Wind FIR BH BPF	262144	14-30	-70.4	2.98	64.5
Wind FIR CH BPF	262144	14-30	-70.4	3.0	64.5
Wind FIR FT BPF	262144	13-30	-69.2	2.33	64.5
Wind FIR KA BPF	262144	20-30	-60.6	3.37	64.5
Wind FIR NU BPF	262144	14-30	-70.3	2.99	64.5
Equir. FIR Multir. HPF	variab.	22-30	-70.3	0.53	1.26
MM Wavlt. BPF	arbitr.	none	-26.8	0.31	0.4

Table 1: ANSI classification and error, mean warble $\overline{W}$ and minimum required room reverberation time at 25 Hz for accurate analysis of actual implementations of different filter banks. BH: Blackman-Harris, CH: Chebyshev, FT: Flat-top, KA: Kaiser, NU: Nuttall. Error threshold for classification is -120 dB.

References

[1] ANSI S1.11-2004, "Specification for octave-band and fractional-octave-band analog and digital filters", *Standards Secretariat, Acoustical Society of America*, (2004)

[2] ISO/FDIS 3382, "Acoustics: Measurement of the Reverberation Time of rooms with reference to other acoustical parameters", *International Organization for Standardization*, (1997)

[3] Brian F. G. Katz, "International Round Robin on Room Acoustical Impulse Response Analysis Software", *Acoustics Research Letters Online, Published Online*, (2004)

[4] F. Jacobsen, "A note on acoustic decay measurement", *Journal of Sound and Vibration 115, 163-170*, (1987)

[5] S-K. Lee, "An acoustic decay measurement base on time-frequency analysis using wavelet transform", *Journal of Sound and Vibration 252(1), 141-153*, (2002)

[6] S-K. Lee, M-S. Lee, "Reverberation time measurement for an acoustic room with low value of BT by utilizing wavelet transform", *Journal of Sound and Vibration 275 1101-1112*, (2004)

[7] Mathworks, Inc., "MATLAB - robust multilinear regression (robustfit)" (2007)